DFT study of oxygen-bridged Zn^{2+} ion pairs in Zn/ZSM-5 zeolites

Alexei L. Yakovlev [a,*], Alexander A. Shubin [b], Georgii M. Zhidomirov [b] and Rutger A. van Santen [a]

[a] *Schuit Institute of Catalysis, Laboratory of Inorganic Chemistry and Catalysis, Eindhoven University of Technology, PO Box 513, 5600MB Eindhoven, The Netherlands*

[b] *Boreskov Institute of Catalysis, SB RAS, pr. Lavrentieva 5, 630090 Novosibirsk, Russia*

Received 13 June 2000; accepted 14 September 2000

A cluster model for Zn/ZSM-5 zeolite is proposed, which consists of an oxygen-bridged $[Zn–O–Zn]^{2+}$ moiety attached to two framework aluminum ions of two adjacent ZSM-5 5-rings. Its stability and catalytic activity in ethane dehydrogenation were considered using the DFT method and compared with those for single Zn^{2+} ions in the same rings. It is shown that the oxygen-bridged Zn^{2+} pair is rather reactive towards ethane dissociation and that the rate-limiting step is release of hydrogen.

Keywords: Zn/ZSM-5, DFT calculations, ethane dehydrogenation

1. Introduction

Since the early studies by Boudart et al. [1–3] the possibility of the formation of redox ion pairs in zeolites by ion exchange has drawn attention. They proposed for the Fe(II)/Fe(III) redox couple in Y zeolite that the redox properties of this binuclear ion system are due to elimination or addition of the bridging oxygen atom in the ion pair system $[Fe–O–Fe]^{4+}$ [3]. The bridging position of the oxygen in the Fe/Y zeolite was confirmed by Mössbauer [3] and IR [4] studies. Another reason for interest in such a species relates to studies of cationic exchange in high-silica zeolites and especially to an understanding of the overexchange phenomenon [5]. A number of studies have been devoted to demonstrate experimentally the existence of $[Cu–O–Cu]^{2+}$ structures in highly loaded Cu/ZSM-5 [5–13]. Redox properties of these species make them active in N_2O decomposition and reduction [14]. The observation of isothermal oscillations of N_2O decomposition over Cu/ZSM-5 catalysts is usually interpreted as a consequence of a change in reductive and oxidative properties of nitrous oxide in the interaction with the $[Cu–O–Cu]^{2+}$ structure as a function of oxygen concentration [15–17]. Recently, considerable attention was paid to studies of the activity of Fe/ZSM-5 zeolites in the selective catalytic reduction of NO_x [18,19] and the binuclear $[HOFe–O–FeOH]^{2+}$ structure was suggested as an active site [19]. XAFS, FTIR, ESR, H_2-TPR and CO-TPR studies supported the hypothesis about the formation of bridged binuclear iron clusters in Fe/ZSM-5 prepared by sublimation of $FeCl_3$ [20,21]. Oscillations of N_2O decomposition were also observed for these catalysts [22]. In this case the oscillations were observed only in the presence of water. Nevertheless, there is evidence that the oscillations are related to chemical transformations of the binuclear $[Fe–O–Fe]^{x+}$ structure in the course of the reaction. Apparently, the binuclear sites are also the cause of the peculiarities of the O_2 isotope exchange in these systems [23], which are not observed in the catalysts prepared by impregnation where the majority of iron is usually present as Fe_2O_3 particles. Studies of the reactivity of the selective oxidation site (α-oxygen), which is formed upon low-temperature N_2O decomposition, lead the authors to relate this to monooxygenase-like behavior for the oxidation of saturated hydrocarbons, in particular methane. By analogy with the known binuclear Fe-containing structure of the active site of MMO the active site in Fe/ZSM-5 has been suggested also to be a binuclear oxo-complex.

The probability of formation of bridged binuclear complexes of exchanged cations is related, in the first place, to the Si/Al ratio and to the nature of Al distribution in the zeolite framework. Experimental observations of such structures in Cu/ZSM-5 and Fe/ZSM-5 lead to the conclusion that this property of the zeolite matrix may also show up in the case of other multi-valent cations.

Recently, Zn-containing zeolites, and especially Zn/ZSM-5, attracted much attention due to their catalytic activity in the reactions of dehydrogenation of light alkanes and aromatization of hydrocarbons [24,25]. Considerable efforts have been devoted to clarifying the structure of the Zn^{2+}-ion oxide species in these systems and to the determination of their catalytically active forms [20,26,27]. Among them the binuclear form $[Zn–O–Zn]^{2+}$ has been proposed [25] to account for the overexchange phenomenon in Zn-exchanged ZSM-5 zeolites. Unfortunately, due to the complexity of the systems, many problems concerning the state and chemical activity of zinc ion species in these zeolite systems remain. Most authors came to the conclusion that the dehydrogenating ability of the Zn component is important in catalytic conversion of alkanes in zeolite systems [24–27]. The role of the zinc ions has been ascribed to an enhancing of the recombination of hydrogen atoms and desorption of H_2 [26,27].

* To whom correspondence should be addressed.

So far, there were very few published studies with calculations of binuclear oxygen-bridged metal complexes in zeolites. First of all, the work of Sayle et al. [28,29] should be mentioned. Low-energy configuration of copper oxide species has been identified by static atomistic simulation techniques. A rather high probability of formation of Cu(II)–OH–Cu(I) bridge structures was found [28] and a detailed analysis of stability and structure of this species was carried out [29]. Teraishi et al. [30] studied the coordination and structure of single Cu ions and binuclear copper species in ZSM-5 zeolite by means of MD and *ab initio* cluster model simulations. Goodman et al. [31] studied chemical reduction of O- and O_2-bridged cations in CuZSM-5 by H_2, CO, and NO, as well as their autoreduction, using simple cluster models and DFT approach. Recently, the stability of the Pd(II)–O–Pd(II) structure in 6-rings of ZSM-5 was studied by Rice et al. [32].

In our previous paper we presented results for the ethane dehydrogenation reaction on a single Zn^{2+} ion attached to a cluster representing a ZSM-5 site [33]. Here we present the results of a theoretical study of the structure and reactivity of binuclear $[Zn–O–Zn]^{2+}$ complexes, as well as single Zn^{2+} ions, in contact with a large cluster geometrically related to the ZSM-5 support. As an example of the alkane activation on this site we have carried out calculations on intermediates of the ethane dehydrogenation reaction.

2. Computation details

The density functional (DF) calculations were performed using the ADF v2.3 package. TZ + VP basis sets were used throughout (type IV basis sets in ADF). Geometry optimization was carried out employing the local density approximation (LDA) [34]. At LDA geometry the energy was computed at GGA level using the exchange–correlation functional of Perdew and Wang [35].

The basic cluster model Z consists of two 5-member rings representing part of the wall of the straight channel of the ZSM-5 structure. The placement of the cluster in ZSM-5 structure can be pictured from figure 1. The nonequivalent lattice positions of silicon atoms in the ZSM-5 structure [36] are shown as Txx. The cluster contains both Si12 and Si9, which are often believed to be locations for silicon substitution by aluminum. H forms of Al-substituted clusters (models Z_sH_2 and Z_dH_2, where the subscript "s" or "d" stands for "same" and "different", respectively, see below) were calculated. In the Z_sH_2 model aluminum ions are placed in the same ring (Si6 and Si12 are substituted) and are separated by one silicon–oxygen tetrahedron, while in Z_dH_2 they are in different rings (Si9 and Si12 are substituted) and are separated by two such tetrahedra. The site Z_sH_2 provides a possibility to replace two charge-compensating protons by one two-valent cation, such as Zn^{2+} (Z_sZn model). In principle, this is also possible for the site Z_dH_2, which was also calculated (Z_dZn model), but the large distance between farthest AlO_4 tetrahedron and Zn^{2+} ion creates an energetically unfavorable charge separation. To avoid this situation, another ZnO molecule may serve as a bridge between these charge centers, resulting in a $[ZnOZn]^{2+}$ moiety as a big counter-ion (Z_dZn_2O model). In principle, it is possible that more ZnO molecules serve as bridges if the separation between framework Al ions is larger.

The interaction of Zn-containing clusters with alkanes was studied using ethane as an example. For the cluster Z_sZn, with only one Zn cation, it was previously found that ethane activation results in a $[ZnC_2H_5]^+$ cation and zeolitic bridging OH group, i.e., the "alkyl route" of the reaction [37]. In contrast to the Z_sZn cluster, ethane dissociation on the cluster Z_dZn_2O may result either in the cluster $Z_d(ZnOH)(ZnC_2H_5)$ or in the cluster $Z_d(H)(ZnOZnC_2H_5)$ or in the cluster $Z_d(Zn(OC_2H_5)ZnH)$. The difference between the first two models is in the place of attachment of the hydrogen atom from the ethane molecule: in the former it is bound to the bridging oxygen between Zn ions, whereas in the latter it is bound to framework oxygen between Al and Si. In the third model ethyl is bound to the extra-lattice bridging oxygen and H is at one of the zinc atoms. We have also calculated models which can be considered as resulting either from ethylene desorption from the previous models or from dissociation of hydrogen on Zn/ZSM-5. These are the $Z_d(ZnOH)(ZnH)$, $Z_d(H)(ZnH)$, and $Z_s(H)(ZnH)$ cluster models, which correspond to Z_dZn_2O, Z_dZn, and Z_sZn substrate clusters, respectively.

In the present calculations we use the cluster approach, where dangling bonds at Si and Al atoms were terminated with hydrogen atoms. The geometry optimization procedure used was as follows. First, the coordinates of all atoms except those of boundary hydrogens were frozen at the lattice positions [36] and for the latter the direction to the absent lattice oxygen was maintained and only T–H bond lengths were varied, where T = Si or Al. For the models Z_sH_2 and Z_dH_2 the coordinates of H atoms of bridging OH groups were also optimized during this step. This procedure was performed only for Z (purely siliceous), Z_sH_2,

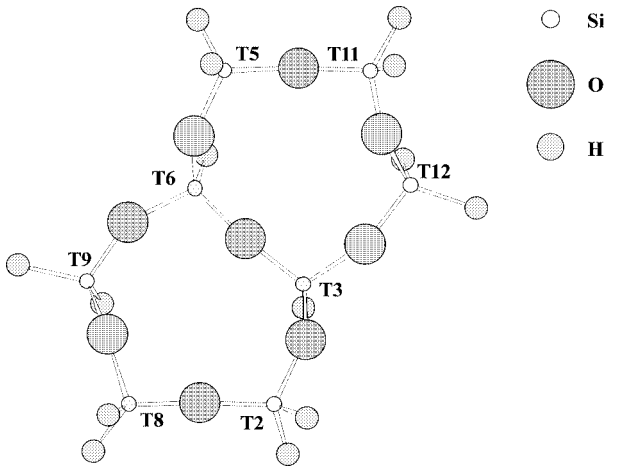

Figure 1. Purely siliceous basic cluster model Z. Crystallographically distinct positions of silicon atoms in ZSM-5 lattice are presented as Txx.

and Z_dH_2 models. For all other models the positions of boundary H atoms were kept fixed either as in the model Z_sH_2 or as in Z_dH_2 depending on the positions of aluminum ions. After that, the Cartesian coordinates of the boundary H atoms were kept frozen and the rest was optimized.

It is important to discuss here the effect of freezing boundary atoms for different models and its dependence on basis sets. We optimized the geometry of the model Z with frozen boundary H atoms using three basis set types: double-ζ (type II in ADF), double-ζ + VP (type III), and triple-ζ + VP (type IV). The optimized Si–O distances are longer than the experimental ones resulting in some shortening of Si–H bonds compared to the previously optimized, which, in turn, results in non-zero forces on the boundary atoms. The magnitude of these forces can be a measure of the "adequateness" of the basis set in question. The comparison shows a substantial decrease (usually by a factor of two) in these forces when a basis set with polarization functions (III or IV) is applied. Therefore, the error introduced by freezing the positions of boundary atoms is smaller with larger basis sets. This was the main reason why we have chosen the type IV basis set in this work.

The largest impact of the freezing of boundary H atoms on accuracy of the results should occur in the case of Al-substituted models because of the significant difference between Al–O distances in $Z_{s,d}X$ models and the corresponding Si–O distances in the Z model. In this case the largest forces are acting on the frozen H atoms bound directly to aluminum. However, the magnitude of the forces is not much larger (approximately by a factor of two) than in the case of the purely siliceous cluster model Z. Besides that, the forces are consistent between different Z_dX and Z_sX models, so that introduced errors are substantially canceled.

3. Results and discussion

In table 1 some resulting distances in the first coordination sphere of zinc after geometry optimization of Zn-exchanged clusters are presented. For atom numbers see the corresponding figures pointed out in the first column.

3.1. Formation of Zn/ZSM-5

Zn/ZSM-5 can be prepared by various means: ion exchange [38], incipient wetness impregnation [26], Zn sublimation [39], $ZnCl_2$ sublimation with subsequent washing [20] or solid-state ion exchange with ZnO [40] or metallic Zn [41]. Since the Zn form of a zeolite may be prepared by deposition of gaseous ZnO onto its H form, it is worthwhile to consider the reaction

$$Z\text{–}H_2 + x\mathrm{ZnO} \rightarrow Z\text{–}\mathrm{Zn}_x\mathrm{O}_{x-1} + \mathrm{H_2O}$$

where in our case $x = 1$ or 2, Z = Z_d, Z_s. The corresponding reaction energies for different x and Z are presented in the table 2 in the rows 2, 9, 10, and 16. Alternatively Z_dZn and Z_sZn can be obtained via reactions 10 and 17, respectively, which represent the formation of Zn/ZSM-5 via interaction of the zeolitic H form with metallic zinc vapor. A few points are worth to be mentioned here. As expected, the stabilization of a single zinc ion in a 5-ring with two Al ions is better than with one. The difference amounts to 30 kcal/mol (compare rows 9 and 16 in table 2). This can be attributed to the effect of unfavorable charge separation due to large distance between the negatively charged remote Al–O tetrahedron and the Zn^{2+} ion in the case of Z_dZn formation. The second ZnO molecule adsorbed on Z_dZn closes this distance, which results in more stable Z_dZn_2O complex. The energy of ZnO adsorption was calculated to -90 kcal/mol, indicating that two ZnO molecules will rather form one Z_dZn_2O site than two separate such as Z_dZn. Another indication of the instability of the Z_dZn site is its reactivity towards water: the energy of reaction 12 (table 2) is -33 kcal/mol. These results indicate that Z_d(H)(ZnOH) will be a primary product when a ZnO molecule reacts with a Z_dH_2 site, the reaction energy being -108 kcal/mol (sum of rows 9 and 12, table 2). Interestingly, this value is close to the energy of reaction 16, the formation of the Z_sZn site. The Z_dZn_2O is also reactive towards water, however in this case the hydration of the site is less exothermic: the energy gain is 24 kcal/mol.

We could not find in the literature any indication about the structure of gaseous zinc oxide. Thus we decided to calculate the relative stability of the intrazeolite particles also to the zinc oxide dimer Zn_2O_2. Since the heat of ZnO dimerization is calculated to be -92.5 kcal/mol, the energy of reaction 2 (table 2) has to be corrected by this value. Thus, the energy of the reaction $Z_dH_2 + Zn_2O_2 \rightarrow Z_dZn_2O + H_2O$ is -73.5 kcal/mol, still very exothermic.

Comparison of the local geometry of Zn ions surrounding in Z_dZn and Z_sZn reveals a few interesting points. As one can expect the zinc ion in the Z_sZn structure is coordinated to four oxygen ions (see table 1 and figure 2). However in the case of Z_dZn, despite the presence of only one Al-centered tetrahedron in the vicinity of the Zn ion, it is also coordinated to four framework oxygens (see table 1 for distances and figure 2 for atom numbering). Interestingly, the distances Zn–$O_{(2)}$ and Zn–$O_{(5)}$ in Z_dZn are as short as in Z_sZn although in Z_dZn the two O ions are bound to silicon not aluminum. This strong Zn–$O_{(2)}$ interaction caused changes in T–O bonds in the chain T_9–$O_{(4)}$–T_6–$O_{(2)}$, namely, T_9–$O_{(4)}$ and T_6–$O_{(2)}$ became longer by 0.15 Å and $O_{(4)}$–T_6 became shorter by 0.08 Å compared to other Al–O and Si–O bonds. Thus, the distortions in the framework bonds facilitate the stabilization of the Zn ion in such an unusual situation.

The most important parameter that correlates with the cations reactivity at different positions is their Lewis acidity. Some calculated quantities, such as the relative position of the lowest unoccupied molecular orbital (LUMO) and formal atomic charges, can give an indication of the strength of the Lewis acid in question. For example, a lower position of the LUMO and higher positive charge correspond to a

Table 1
Optimized interatomic distances in the first coordination sphere of zinc ions ($R < 2.5$ Å) for all calculated Zn-containing models. For atom numbers see corresponding figures pointed out in the first column.

Model	Interatomic distances at Zn (Å)			
Z_sZn	Zn–O_2	1.93	Zn–O_5	2.04
figure 2	Zn–O_3	1.92	Zn–O_6	2.03
Z_dZn	Zn–O_2	1.93	Zn–O_5	2.28
	Zn–O_3	1.95	Zn–O_6	1.92
Z_dZn_2O	Zn_1–O_2	2.18	Zn_2–O_5	2.16
figure 3	Zn_1–O_3	2.00	Zn_2–O_7	1.94
	Zn_1–O_6	2.03	Zn_2–O_9	2.43
	Zn_1–O_{10}	1.83	Zn_2–O_{10}	1.79
$Z_s(H)(ZnC_2H_5)$	Zn–O_3	2.04	Zn–C_1	1.92
figure 4	Zn–O_6	1.96		
$Z_d(H)(ZnC_2H_5)$	Zn–O_3	2.07	Zn–C_1	1.92
	Zn–O_6	1.96		
$Z_d(ZnOH)(ZnC_2H_5)$	Zn_1–O_3	2.05	Zn_2–O_4	2.19
figure 5	Zn_1–O_6	1.95	Zn_2–O_5	2.15
	Zn_1–C_1	1.91	Zn_2–O_7	1.94
			Zn_2–O_{10}	1.80
$Z_d(H)(ZnOZnC_2H_5)$	Zn_1–O_3	2.23	Zn_2–O_5	2.17
figure 6	Zn_1–O_6	2.02	Zn_2–O_7	1.93
	Zn_1–O_{10}	2.10	Zn_2–O_9	2.23
	Zn_1–C_1	1.97	Zn_2–O_{10}	1.79
$Z_d(Zn(OC_2H_5)ZnH)$	Zn_1–O_2	2.16	Zn_2–O_4	2.22
	Zn_1–O_6	1.97	Zn_2–O_5	1.93
	Zn_1–O_{10}	2.05	Zn_2–O_7	1.90
	Zn_1–H	1.54	Zn_2–O_9	2.25
			Zn_2–O_{10}	1.84
$Z_s(H)(ZnH)$	Zn–O_3	2.01	Zn–H_1	1.52
figure 7	Zn–O_6	1.97		
$Z_d(H)(ZnH)$	Zn–O_3	2.00	Zn–H_1	1.50
	Zn–O_6	1.94		
$Z_d(ZnOH)(ZnH)$	Zn_1–O_2	2.49	Zn_2–O_4	2.15
figure 8	Zn_1–O_3	2.26	Zn_2–O_5	2.24
	Zn_1–O_6	2.03	Zn_2–O_7	1.90
	Zn_1–O_{10}	2.29	Zn_2–O_{10}	1.82
	Zn_1–H_1	1.54		

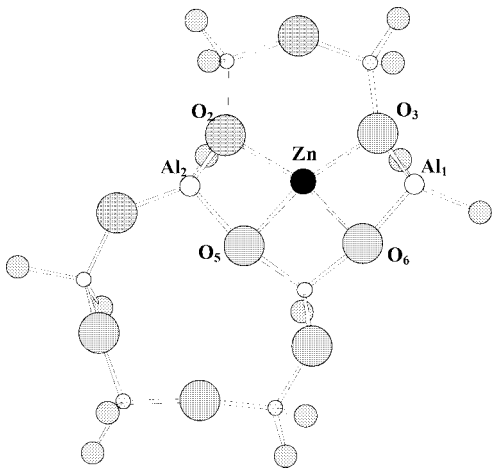

Figure 2. The cluster model Z_sZn in which Al substitutes Si at T12 and T6. Zn^{2+} is used as a counter-ion.

Table 2
Calculated reaction energies of steps of the active sites formation and ethane dehydrogenation.

No.	Reaction	ΔE (reaction) (kcal/mol)
1	$Z_dH_2 + 2ZnCl_2 \rightarrow Z_d(ZnCl)_2 + 2HCl$	34
2	$Z_dH_2 + 2ZnO \rightarrow Z_dZn_2O + H_2O$	−166
3	$Z_dZn_2O + H_2O \rightarrow Z_d(ZnOH)(ZnOH)$	−24
4	$Z_dZn_2O + C_2H_6 \rightarrow Z_d(ZnOH)(ZnC_2H_5)$	−18
5	$Z_dZn_2O + C_2H_6 \rightarrow Z_d(H)(ZnOZnC_2H_5)$	28
6	$Z_dZn_2O + C_2H_6 \rightarrow Z_d(Zn(OC_2H_5)ZnH)$	37
7	$Z_d(ZnOH)(ZnC_2H_5) \rightarrow Z_d(ZnOH)(ZnH) + C_2H_4$	20
8	$Z_d(ZnOH)(ZnH) \rightarrow Z_dZn_2O + H_2$	38
9	$Z_dH_2 + ZnO \rightarrow Z_dZn + H_2O$	−75
10	$Z_dZn + ZnO \rightarrow Z_dZn_2O$	−91
11	$Z_dH_2 + Zn \rightarrow Z_dZn + H_2$	10
12	$Z_dZn + H_2O \rightarrow Z_d(H)(ZnOH)$	−33
13	$Z_dZn + C_2H_6 \rightarrow Z_d(H)(ZnC_2H_5)$	−26
14	$Z_d(H)(ZnC_2H_5) \rightarrow Z_d(H)(ZnH) + C_2H_4$	34
15	$Z_d(H)(ZnH) \rightarrow Z_dZn + H_2$	33
16	$Z_sH_2 + ZnO \rightarrow Z_sZn + H_2O$	−105
17	$Z_sH_2 + Zn \rightarrow Z_sZn + H_2$	−19
18	$Z_sZn + C_2H_6 \rightarrow Z_s(H)(ZnC_2H_5)$	7
19	$Z_s(H)(ZnC_2H_5) \rightarrow Z_s(H)(ZnH) + C_2H_4$	27
20	$Z_s(H)(ZnH) \rightarrow Z_sZn + H_2$	7

stronger Lewis acid site in a row of similar sites. Calculated LUMO energies for Z_dZn_2O (−2.8 eV), Z_sZn (−3.2 eV), and Z_dZn (−4.1 eV) clearly indicate that Lewis acidity strongly increases in this order. Mulliken charges on Zn ions for Z_dZn_2O (0.78 a.u.) and Z_sZn (0.87 a.u.) correlate with a LUMO position. Surprisingly, the Zn formal charge in the Z_dZn cluster is of the same magnitude as in Z_sZn (0.87 a.u.). This also shows the unusual electronic properties of this site.

3.2. Reactivity

As a test of reactivity of the sites we calculated intermediates of the ethane dehydrogenation reaction according to the mechanism proposed in [42] based on the kinetic data analysis. DFT modeling of this mechanism was previously reported for the case of Zn^{2+} in a zeolitic 4-ring [37]. The mechanism comprises the alkane dissociative adsorption, alkene desorption, and hydrogen recombination and desorption with restoration of the initial site, in this order. The energies of dissociative adsorption of ethane and hydrogen molecules on the sites are presented in table 2 and clearly shows the activity dependence on stability of the sites in the row Z_sZn, Z_dZn_2O, and Z_dZn. The most stable Zn^{2+} ion in the cationic position of the 5-membered ring reveals an energetic effect, which qualitatively agrees (taking into account larger basis sets used in this work) with that previously found for different Zn-containing 5-membered rings in the ZSM-5 structure [33]. In contrast to this site the binuclear structure Z_dZn_2O is much more active in these reactions due to substantially higher basicity

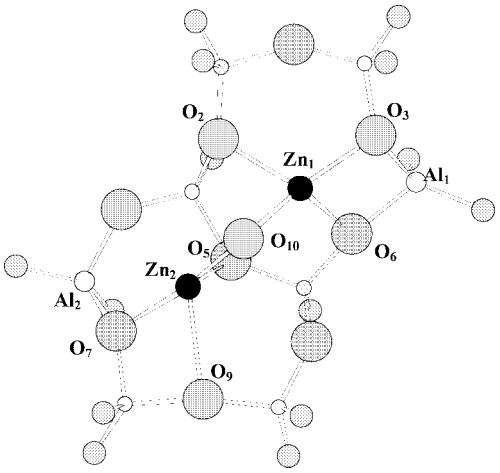

Figure 3. The cluster model Z_dZn_2O in which Al substitutes Si at T12 and T9. $[ZnOZn]^{2+}$ is used as a counter-ion.

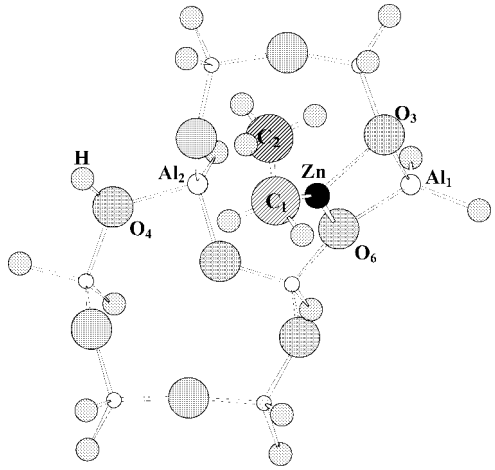

Figure 4. The cluster $Z_s(H)(ZnC_2H_5)$ resulted from dissociation of a C_2H_6 molecule on the cluster Z_sZn.

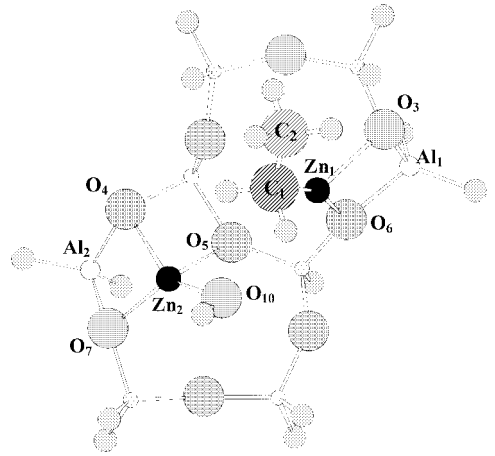

Figure 5. The cluster $Z_d(ZnOH)(ZnC_2H_5)$ resulted from dissociation of a C_2H_6 molecule on the cluster Z_dZn_2O.

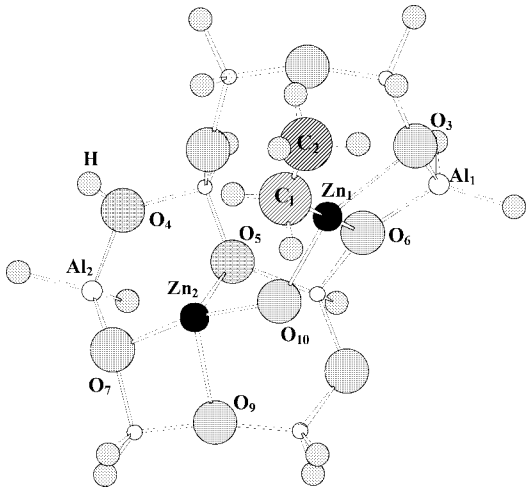

Figure 6. The cluster $Z_d(H)(ZnOZnC_2H_5)$ resulted from dissociation of a C_2H_6 molecule on the cluster Z_dZn_2O.

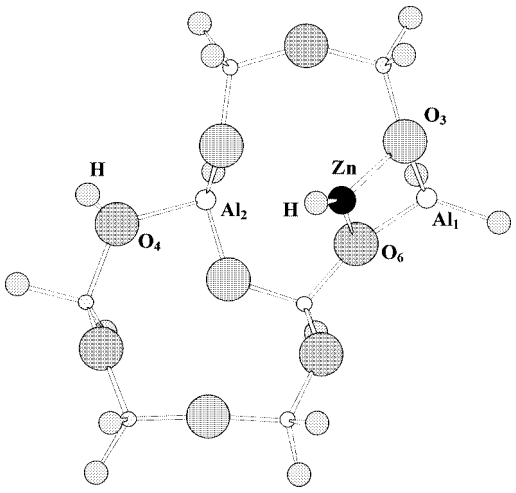

Figure 7. The cluster $Z_d(H)(ZnH)$ resulted from dissociation of an H_2 molecule on the cluster Z_dZn.

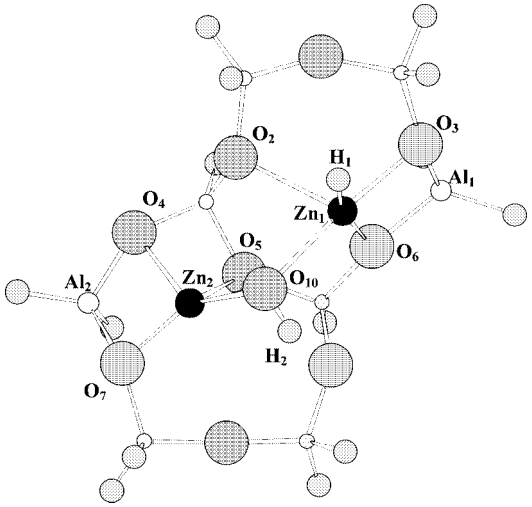

Figure 8. The cluster $Z_d(ZnOH)(ZnH)$ resulted from dissociation of a C_2H_6 molecule on the cluster Z_dZn_2O.

of the extra-lattice oxygen compared to framework O ions. The difference in Mulliken charges between them is about 0.2 a.u. This results in exothermicity of ethane and hydrogen dissociation giving $Z_d(ZnOH)(ZnC_2H_5)$ (table 2, reaction 4) and $Z_d(ZnOH)(ZnH)$ (table 2, reverse reaction 8). It is essential that the alternative "carbanion" route in the ethane dissociation with the formation of $Z_d(Zn(OC_2H_5)ZnH)$, reaction 6, is unfavorable. The routes of ethane dissociation preserving ZnOZn fragment with formation of $ZnOZnC_2H_5$ or ZnOZnH structures are also unfavorable, see for example reaction 5. The unstable site Z_dZn reveals a further increase in the activity in dissociative adsorption of ethane and hydrogen.

Ethylene elimination, as well as subsequent hydrogen recombination closing the catalytic cycle ethane dehydrogenation, are endothermic for all considered sites (reactions 7, l4, 19, and 8, 15, 20, respectively). Formation of ethene from ethane is least unfavorable on a Z_dZn_2O center, but desorption of hydrogen for this site is the most difficult. For Z_dZn both these reaction steps are strongly unfavorable.

As was found in this study, the energetically most unfavorable step in ethane dehydrogenation reaction on oxygen-bridged Zn–O–Zn ion pair sites is hydrogen removal. The same was concluded by Bell et al. for alkane dehydrogenation on a $ZGa(OH)_2$ site in Ga-ZSM-5 [43]. The authors [43] suggested a substitution reaction as the final step of the catalytic cycle. For the case of Zn-ZSM-5 it can be written as follows:

$$Z_d(ZnOH)(ZnH) + C_2H_6 \rightarrow Z_d(ZnOH)(ZnC_2H_5) + H_2$$

and one of the further processes may be

$$Z_d(ZnOH)(ZnC_2H_5) + C_2H_6 \rightarrow Z_d(ZnOC_2H_5)(ZnC_2H_5) + H_2$$

which opens the path for the oligomerisation process.

4. Conclusions

For high-silica zeolites with homogeneous aluminum distribution the probability to find two Al ions in one ring is low. Thus the structures including two Al ions in adjacent rings must be of importance. A cluster model Z_d consisting of two 5-rings with one T atom in each ring substituted by aluminum is proposed. The model represents a fragment of the wall of a ZSM-5 straight channel. The structure of a zinc cation in this position, the Z_dZn model, was calculated using the DFT approach. A remarkably low stability of this cluster, compared to that with two Al ions in one ring (Z_sZn model), was found. The Z_dZn structure is strongly inclined to form oxygen-bridged $[Zn–O–Zn]^{2+}$ cation (Z_dZn_2O structure).

The Z_dZn_2O site is rather reactive towards water, hydrogen, and ethane dissociation. Comparison of different products of ethane dissociative adsorption on Z_dZn_2O showed that formation of the $Z_d(ZnOH)(ZnC_2H_5)$ product is most favorable. Subsequent steps of ethane dehydrogenation on Z_dZn_2O were studied and it was concluded that the most difficult step is the release of hydrogen. In parallel with Bell et al. [43] we suggest that the substitution mechanism of the hydrogen removal should play a role. Similar results were obtained for the Z_dZn model: ethane dissociation is very exothermic, even more than in the case of Z_dZn_2O, hydrogen desorption is very endothermic, and, unlike the Z_dZn_2O case, ethylene desorption is also very endothermic. The calculations for the Z_sZn model are in qualitative agreement with our previous results [33] for ethane dehydrogenation on Zn^{2+} stabilized in one zeolitic ring.

Acknowledgement

The financial support from Dutch Science Foundation in the collaborative Russian–Dutch research project 047-005-011 NWO is gratefully acknowledged.

References

[1] M. Boudart, R.L. Garten and W.N. Delgass, J. Phys. Chem. 73 (1969) 2970.
[2] W.N. Delgass, R.L. Garten and M. Boudart, J. Chem. Phys. 50 (1969) 4603.
[3] R.L. Garten, W.N. Delgass and M. Boudart, J. Catal. 18 (1970) 90.
[4] R.A. Dalla Betta, R.L. Garten and M. Boudart, J. Catal. 41 (1976) 40.
[5] J. Valyon and W.K. Hall, J. Phys. Chem. 97 (1992) 7054.
[6] H. Hamada, N. Matsubayashi, H. Shimada, Y. Kintaichi, T. Ito and A. Nishijima, Catal. Lett. 5 (1990) 189.
[7] W. Grünert, N.W. Hayes, R.W. Joyner, E.S. Shpiro, M.R.H. Siddiqui and G.N. Baeva, J. Phys. Chem. 98 (1991) 10832.
[8] M. Ivamoto, H. Yahiro, K. Tanda, N. Mizuno, Y. Mine and S. Kagawa, J. Phys. Chem. 95 (1991) 3727.
[9] M.C. Campa, V. Indovina, G. Minelli, G. Moretti, I. Pettiti, P. Porta and A. Riccio, Catal. Lett. 23 (1994) 141.
[10] G. Moretti, Catal. Lett. 23 (1994) 135.
[11] J. Sárkány, J.L. d'ltri and W.M.H. Sachtler, Catal. Lett. 16 (1992) 241.
[12] T. Beutel, J. Sárkány, G.D. Lei, J.Y. Yan and W.M.H. Sachtler, J. Phys. Chem. 100 (1996) 845.
[13] J.Y. Yan, G.D. Lei, W.M.H. Sachtler and H.H. Kung, J. Catal. 161 (1996) 43.
[14] F. Kapteijn, J. Rodrigues-Mirasol and J.A. Moulijn, Appl. Catal. B 9 (1996) 25.
[15] H.-G. Lintz and T. Turek, Catal. Lett. 30 (1995) 313.
[16] P. Ciambelli, E. Garufi, R. Pirone, G. Russo and F. Santagata, Appl. Catal. B 8 (1996) 333.
[17] P. Ciambelli, A. Di Benedetto, E. Garufi, R. Pirone and G. Russo, J. Catal. 175 (1998) 161.
[18] X. Feng and W.K. Hall, J. Catal. 166 (1997) 368.
[19] H.-Y. Chen and W.M.H. Sachtler, Catal. Today 42 (1998) 73.
[20] A.A. Battiston, J.H. Bitter and D.C. Koningsberger, Catal. Lett. 66 (2000) 75.
[21] El-M. El-MaIki, R.A. van Santen and W.M.H. Sachtler, J. Phys. Chem. B 103 (1999) 4611.
[22] El-M. El-MaIki, R.A. van Santen and W.M.H. Sachtler, Micropor. Mesopor. Mater. 35–36 (2000) 235.
[23] T.V. Voskoboinikov, H.-Y. Chen and W.M.H. Sachtler, J. Mol. Catal. A 155 (2000) 155.
[24] T. Mole, J.R. Anderson and G. Creer, Appl. Catal. 17 (1985) 141.

[25] Y. Ono, Catal. Rev. Sci. Eng. 34 (1992) 179.
[26] J.A. Biscardi, G.D. Meitzner and E. Iglesia, J. Catal. 179 (1998) 192.
[27] J.A. Biscardi and E. Iglesia, Catal. Today 31 (1996) 207.
[28] D.C. Sayle, C.R.A. Catlow, M.-A. Perrin and P. Nortier, J. Phys. Chem. A 101 (1997) 3337.
[29] D.C. Sayle, C. Richard, C.R.A. Catlow, M.-A. Perrin and P. Nortier, Micropor. Mesopor. Mater. 20 (1998) 259.
[30] K. Teraishi, M. Ishida, J. Irisava, M. Kume, Y. Takahashi, T. Nakano, H. Nakamura and A. Miyamoto, J. Phys. Chem. B 101 (1997) 8079.
[31] B.R. Goodman, W.F. Schneider, K.C. Hass and J.B. Adams, Catal. Lett. 56 (1998) 183.
[32] M.R. Rice, N.O. Gonzales, A.K. Chakraborty and A.T. Bell, in: *Proc. 12th Int. Conf. on Zeolites*, Baltimore, 1998, p. 393.
[33] A.A. Shubin, G.M. Zhidomirov, A.L. Yakovlev and R.A. van Santen, J. Phys. Chem., submitted.
[34] S.H. Vosko, L. Wilk and M. Nusair, Canad. J. Phys. 58 (1980) 1200.
[35] J.P. Perdew and Y. Wang, Phys. Rev. B 45 (1992) 13244.
[36] H. Lermer, M. Draeger, J. Steffen and K.K. Unger, Zeolites 5 (1985) 131.
[37] M.V. Frash and R.A. van Santen, Phys. Chem. Chem. Phys. 2 (2000) 1085.
[38] V.B. Kazansky, V.Yu. Borovkov, A.I. Serykh, R.A. van Santen and P.J. Stobbelaar, Phys. Chem. Chem. Phys. 1 (1999) 2881.
[39] A. Seidel, F. Rittner and B. Boddenberg, J. Phys. Chem. B 102 (1998) 7176.
[40] K. Osako, K. Nakashiro and Y. Ono, Bull. Chem. Soc. Jpn. 66 (1993) 755.
[41] H.K. Beyer, G. Pál-Borbély and M. Keindl, Micropor. Mesopor. Mater. 31 (1999) 333.
[42] B.-Z. Wan and H.M. Chu, J. Chem. Soc. Faraday Trans. 88 (1992) 2943.
[43] N.O. Gonzales, A.K. Chakraborty and A.T. Bell, Topics Catal. 9 (1999) 207.